Progress In Electromagnetics Research C, Vol. 115, 205–217, 2021

Behavioral Modeling for Nonlinear Effects of Receiver Front-Ends Based on Block-Oriented Structures

Chongchong Chen, Hongmin Lu*, Yu Zhang, and Guangshuo Zhang

Abstract—In this paper, a novel behavioral model for the receiver front-end is presented. This model allows the accurate prediction of the nonlinear effects of the receiver front-end including the in-band distortion, intermodulation, and harmonic generation. The behavioral model is a block-oriented model that consists of three blocks, the frequency conversion block, nonlinear block, and memory linear block. The nonlinear block and memory linear block are represented by the polynomials in time domain, respectively, which can characterize the high-order nonlinearities and strong memory effects by the appropriate adjustment of the polynomial order. An original model parameter identification procedure that can efficiently estimate the model parameters by using the specific input-output data is also proposed. Moreover, the presented behavioral model and identification procedure are assessed by the experiment with the excitation of single-tone signals, multitone signals, and WCDMA signals, respectively. The comparison between the measurement and model simulation suggests that the behavioral model has good accuracy of the prediction of the nonlinear effects of the receiver front-end.

1. INTRODUCTION

With the prosperity and development of wireless communication technology, the electromagnetic environment has become increasingly complex. The complex electromagnetic environment that contains many interference signals may seriously affect the performance of communication equipments and result in the deterioration of communication quality, such as the high data error rate of communication receivers, the false indicator information of navigation systems, and the reduction of detection accuracy of radar receivers. In fact, these unexpected phenomenon mostly results from the nonlinear effect of receivers, such as desensitization, blocking, intermodulation, cross-modulation, and reciprocal mixing, which may cause signal distortion and the degradation of the spurious-free dynamic range (SFDR) of receivers. In order to predict the nonlinear effect of receivers in the complex electromagnetic environment and evaluate the receiver performance, it is of great significance to carry out a study of the nonlinear behavioral model of receivers.

Generally, the nonlinear effects of receivers mainly derive from the receiver front-end that contains many nonlinear analog devices and circuits. The receiver front-end is in the principle of heterodyne to transform the radio frequency (RF) input signals into intermediate frequency (IF) signals or baseband signals. In the front-end, the signals from the antenna port will be filtered, amplified, and converted to IF signals. The structure of receiver front-end is the cascade of nonlinear components such as filters, amplifiers, and mixers, as shown in Fig. 1. It is well known that the amplifiers and mixers are composed of nonlinear devices such as transistors and the circuit with capacitors and inductors, which have strong nonlinearities and memory effects [1–4]. Due to the characteristic of transistors, the nonlinearity of the amplifier is closely related to the power of input signals. A large power signal will make the amplifier work in the nonlinear region or the saturated region, which produces the nonlinear effects of the gain

Received 8 July 2021, Accepted 13 September 2021, Scheduled 25 September 2021
* Corresponding author: Hongmin Lu (hmlu@mail.xidian.edu.cn).
The authors are with the School of Electronic Engineering, Xidain University, China.

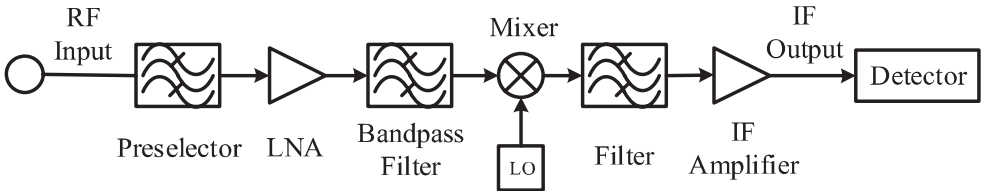

Figure 1. Structure of receiver front-ends.

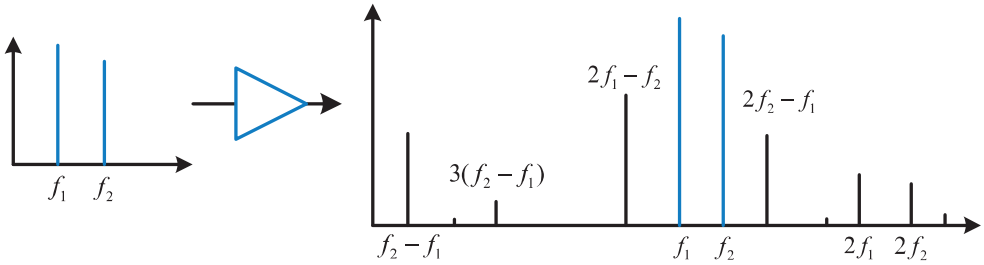

Figure 2. Nonlinearities of amplifiers.

compression and intermodulation among the input signals and leads to the spectral regrowth, as shown in Fig. 2. Moreover, the signal leakage among the mixer ports may also result in many harmonics and intermodulation products in the output of the mixer [5, 6].

For the memory effect, it is said that the output depends on not only the value of the current input but also the past input, even the past values of the output itself [7]. In the receiver front-end, the memory effects are mainly derived from the filters, matching network, and bias circuits of the nonlinear components. In [2], Vuolevi et al. suggested that memory effect can be divided into electric memory effect and thermal memory effect. The electric memory effect is mainly caused by capacitors, inductors, and energy storage components, and the thermal memory effect is related to the thermal effects of active devices. The memory effect makes the nonlinear effects closely related to the frequency and envelope bandwidth of the input signals.

The nonlinearity of the whole receiver front-end can be viewed as the cascade of nonlinearities of each component, which is quite complex. As shown Fig. 3, the cascade of nonlinearities of the receiver front-end is depicted. The input signals contain not only the desired signals but also plenty of in-band

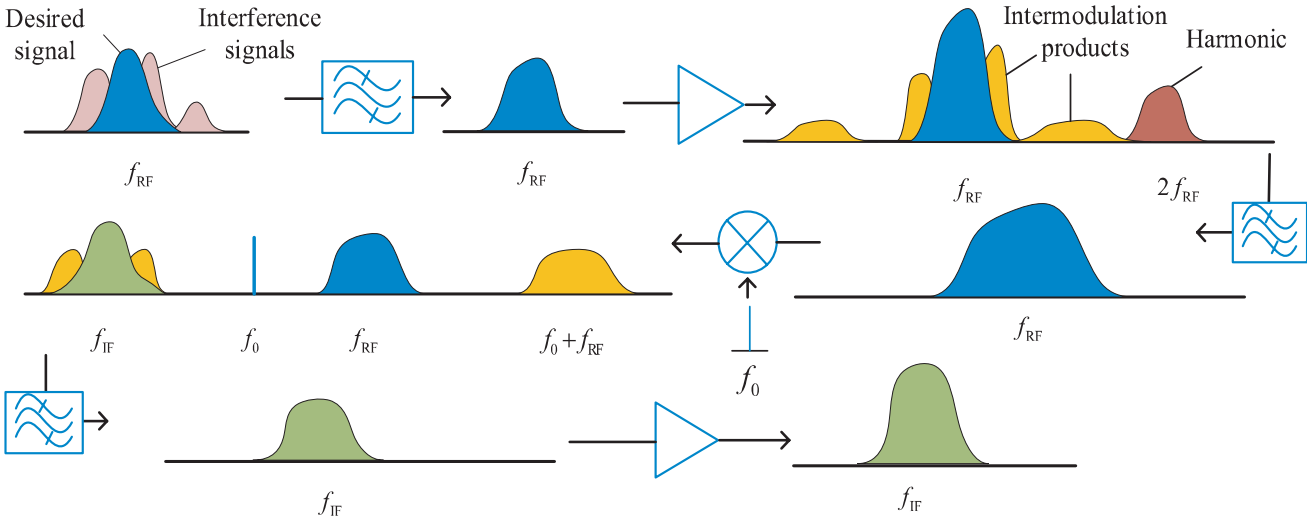

Figure 3. Cascade of nonlinearities of receiver front-ends.

and out-of-band interference signals. The preselector can restrain the most of out-of-band interference signals but cannot completely eliminate the out-of-band signals with high power and in-band interference signals. Hence, due to the nonlinear effects and memory effects of the amplifiers, mixers, and filters, lots of harmonics and intermodulation products among the desired signals and the interference signals are generated. Once these nonlinear products fall into the IF output passband of the receiver front-end, which will result in the noise interference and the signal distortions.

Because of the nonlinearities and memory effects of the components of the receiver front-end, the receiver can be viewed as complex nonlinear system with memory. To analyze the nonlinearity of the receiver, either the approach of experimental measurement or circuit-level simulation demands long time consumption and high computation resource. The behavioral model is an effective scientific approach for the study of complex nonlinear systems and has been widely applied to the research on the nonlinearities and memory effects of RF nonlinear devices, such as amplifiers [8–10] and mixers [4, 6, 11]. Besides, these models have been widely used in the study of behavioral model of nonlinear systems and devices [12–15].

For the receiver front-end, most of the research is mainly about its nonlinearities, the research on the behavioral model of its whole structure is few. In [16], Grimm et al. analyzed the nonlinear effects in the direct frequency conversion receiver in detail, including RF nonlinearity, IQ mixer nonlinearity, and baseband nonlinearity, and proposed a cascade structure of three nonlinear polynomials of power series to characterize these nonlinearities. Due to the interaction between parameters of the nonlinear polynomials of the cascade structure, the identification of the parameters is compliable and requires large amount of computation. Hence, it is not suitable for the analysis of high-order nonlinearities and strong memory effects.

In this paper, a nonlinear behavioral model for the receiver front-end is proposed, which is capable of the prediction of nonlinear effects including signal distortion, intermodulation, and spurious response under a certain electromagnetic environment. On the basis of the nonlinear characteristics of the receiver front-end, this behavioral model is a block-oriented model constructed by three blocks, the frequency conversion block, nonlinear block, and memory linear block. The nonlinear block and memory linear block are expressed by nonlinear polynomials in the time domain, and it can characterize the high-order nonlinearities and strong memory effects by adjusting the polynomial order. The modeling procedure of the nonlinear behavioral model is specified in Section 2. In Section 3, the identification method is put forward based on the prior knowledge of the receiver front-end, and the parameters of the nonlinear block and memory linear block are identified separately with specific input-output signals, which makes the identification process more efficient and accurate for the high-order behavioral model. In Section 4, the validation of the nonlinear behavioral model is carried out in the experiment, and the accuracy of the behavior model is analyzed with the experimental test of single-tone signals, multitone signals, and WCDMA signals, respectively.

2. BEHAVIORAL MODEL STRUCTURE

Since the complex nonlinearities and memory effects of the receiver front-end, we consider the whole receiver front-end as a black box model and establish the nonlinear behavioral model by using the measured input-output data. According to the system identification theory and the characteristics of the receiver front-end, the behavioral model is constructed from three parts: the frequency conversion block, nonlinear block, and memory linear block, which represent the frequency conversion function, nonlinearities, and memory effects of the front-end, respectively.

For the frequency conversion function, one or more mixers are applied in the receiver front-end to transform the RF signals into signals of the desired frequency. However, when the mixer implements the frequency conversion function, it also brings about lots of nonlinearities [4–6]. It is worth noting that the frequency conversion block is not to represent a certain mixer of the RF front-end, but the frequency conversion function. Therefore, the frequency conversion block can be expressed as a down-converter, as shown in Fig. 4, where $x(t)$ is the complex RF input signal, and ω_0 is the tuning local oscillation frequency of the front-end. The nonlinear block is to characterize the nonlinearities of the whole receiver front-end, and it can be expressed as a nonlinear function, such as the power series, the Bessel series or Chebyshev polynomial series. Usually, the power series is used as a mathematical model to analyze the

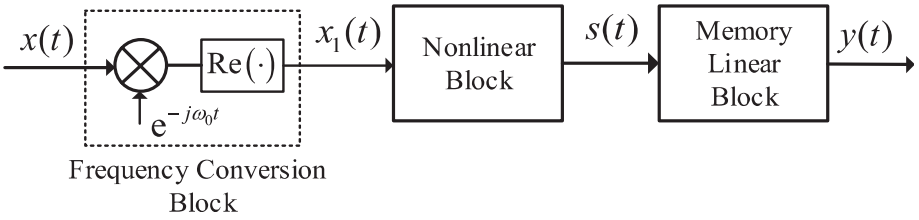

Figure 4. Behavior model of receiver front-ends.

nonlinear characteristics of various devices, because of the simplicity of the coefficient identification. In this paper, the power series is used to express the nonlinear block, and the expression can be written as

$$s = F\left[x_1(t)\right] = \sum_{i=1}^{N} a_i {x_1}^i(t) \tag{1}$$

The function $F(\cdot)$ denotes the nonlinear function; N denotes the order of nonlinear block; and a_i is the nonlinear parameter. The memory linear block represents the memory effects of the receiver front-end. Due to the memory effects, the output is much related with not only the instantaneous input but also the past input signals; therefore, the memory linear block can be formulated as

$$y(t) = \sum_{m=0}^{M-1} b_m s(t - \tau_m) \tag{2}$$

where M denotes the depth of the memory effect, and b_m is the linear parameter. By using Eqs. (1) and (2), the relationship between the input signal and output signal of the behavioral model is obtained as Eq. (3). Thus, the behavioral model is constructed based on polynomials in the discrete time domain, as shown in Fig. 5. The identification process is to estimate parameters a_i of the nonlinear block and the parameters b_m of the linear block.

$$y(n) = \sum_{m=0}^{M-1} b_m \sum_{i=1}^{N} a_i {x_1}^i(n-\mathrm{m}) = \sum_{m=0}^{M-1} \sum_{i=1}^{N} a_i b_m {x_1}^i(n-\mathrm{m}) \tag{3}$$

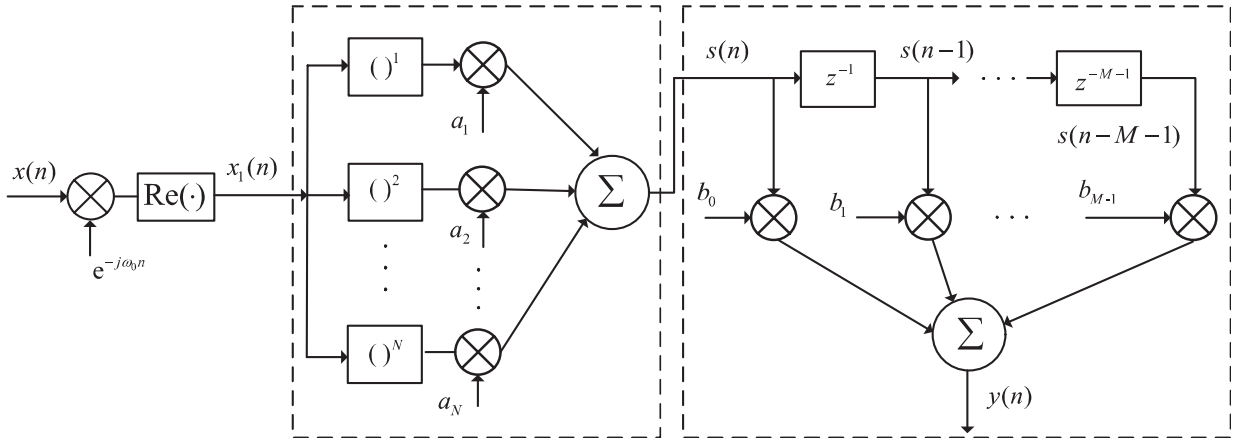

Figure 5. Diagram of the behavioral model.

3. PARAMETER IDENTIFICATION

As shown in Eq. (3) and Fig. 5, the interaction between the parameters a_i and b_m is quite intricate. Though there are some methods that can directly estimate the parameters by using the input and

output testing data, those also require a good deal of optimization procedure and computation. The accuracy is much related with the measured input-output data. However, the prior knowledge of the receiver will be of great help to the parameter identification of the behavior model. In this section, based on the priori knowledge of the receiver front-end, a two-step identification method is proposed to identify the parameters of the behavioral model by using the experimental input-output measurements.

3.1. Identification of Linear Block

It is known that the nonlinear effects of the receiver front-end are mostly derived from the amplifiers and mixers. On the one hand, the nonlinearities are much related to the power of input signals, and the signal with large power could make the nonlinear components inside the receiver front-end work in nonlinear region or saturation region and leads to the nonlinear effects. On the other hand, the memory effect is closely associated with the envelope bandwidth of the input signals. Therefore, the sufficient small signal with wideband modulation is used as the input signal to identify the parameters b_m of the linear block, which can make the receiver work in linear region to avoid the disturbance of the nonlinearities and generate the output data without nonlinearities but memory effects [11]. Assume that the input signal is a modulated signal with RF carrier $\tilde{x}(n) = \tilde{A}_{\mathrm{s}}(n)\mathrm{e}^{j\omega_{\mathrm{c}}n}$, where $\tilde{A}_{\mathrm{s}}(t)$ is the complex envelope that has small amplitude; the wide bandwidth that covers the whole output bandwidth of the front-end; and ω_{c} is the carrier frequency. After the process of the conversion block, the signal x_1 can be written as

$$x_1(n) = \mathrm{Re}\left\{\tilde{A}_{\mathrm{s}}(n)\mathrm{e}^{j\omega_{\mathrm{c}}n}\mathrm{e}^{-j\omega_0 n}\right\} = \mathrm{Re}\left\{A_{\mathrm{s}}(n)\mathrm{e}^{j\varphi(n)}\mathrm{e}^{j\omega_{\mathrm{c}}n}\mathrm{e}^{-j\omega_0 n}\right\} = A_{\mathrm{s}}(n)\cos((\omega_{\mathrm{c}}-\omega_0)n+\varphi(n)) \quad (4)$$

where $A_{\mathrm{s}}(n)$ is the small amplitude of the envelope, and $\varphi(n)$ is the phase of the envelope. Because of the small input power that could make the receiver work in the linear region, the output signal of the nonlinear block can be simplified as

$$s(n) = \sum_{i=1}^{N} a_i {x_1}^i(n) \approx a_1 x_1(n) = a_1 A_{\mathrm{s}}(n)\cos((\omega_{\mathrm{c}}-\omega_0)n+\varphi(n)) \quad (5)$$

According to Eq. (2), the expression of the linear block in the frequency domain can be expressed as

$$Y(\omega) = \sum_{m=0}^{M-1} b_m S(\omega)\,\mathrm{e}^{-j\omega m} = H(\omega)S(\omega) \quad (6)$$

where $H(\omega) = \sum_{m=0}^{M-1} b_m \mathrm{e}^{-j\omega m}$ can be considered as the Fourier transform of the sequence $\{b_m\}(m = 1, 2, 3, \ldots, M-1)$. Combining Eqs. (5) and (6), we can obtain

$$H(\omega) = \frac{Y(\omega)}{S(\omega)} = \frac{Y(\omega)}{a_1 X_1(\omega+\omega_0)} \quad (7)$$

where $X_1(\omega+\omega_0)$ and $Y(\omega)$ can be obtained from the Fourier transformation of the input and output data. Therefore, the parameter b_m of the linear block can be estimated by the mean-squared-error cost function in Eq. (8) with the optimization of the depth of the memory M.

$$\begin{aligned} \hat{\mathbf{b}} &= \underset{\mathbf{b},M}{\mathrm{argmin}} \|\boldsymbol{\varepsilon}\|^2 \\ \varepsilon(\omega) &= \left| H(\omega) - \sum_{m=0}^{M-1} b_m \mathrm{e}^{-j\omega m} \right| \\ \mathbf{b} &= [b_0, b_1, \ldots, b_{M-1}]\,;\ \boldsymbol{\varepsilon} = [\varepsilon(\omega_1), \varepsilon(\omega_2), \ldots, \varepsilon(\omega_N)] \end{aligned} \quad (8)$$

3.2. Identification of Nonlinear Block

For the nonlinear block, it is expressed by nonlinear function of power series, as shown in Eq. (9)

$$y = a_1 x + a_2 x^2 + a_3 x^3 + \dots \tag{9}$$

Assume that the input is a single tone signal $x = A\cos(\omega t)$, then the output of the nonlinear block can be written as (expansion in the order of 5)

$$\begin{aligned} y &= a_1 A\cos(\omega t) + a_2 A^2\cos^2(\omega t) + a_3 A^3\cos^3(\omega t) + a_4 A^4\cos^4(\omega t) + a_5 A^5\cos^5(\omega t) + \dots \\ &= \frac{1}{2}a_2 A^2 + \frac{3}{8}a_4 A^4 + \left(a_1 A + \frac{3}{4}a_3 A^3 + \frac{5}{8}a_5 A^5\right)\cos(\omega t) + \left(\frac{1}{2}a_2 A^2 + \frac{1}{2}a_4 A^4\right)\cos(2\omega t) + \dots \end{aligned} \tag{10}$$

We can observe that the output of the nonlinear block has not only the distorted fundamental component but also the DC and many high-order harmonic components. Though the receiver front-end may give rise to lots of nonlinear products, many of them will be filtered because of the limitation of its output bandwidth, which lead to that the obtained output data contains only part of the nonlinear products. Therefore, the output data with part of nonlinearities will be used to identify the nonlinear parameters. In the meantime, as shown in Eq. (10), the fundamental term $(a_1 A + 3/4 a_3 A^3 + 5/8 a_5 A^5)\cos(\omega t)$ contains the odd order nonlinear products, while the term of second harmonic $(1/2 a_2 A^2 + 1/2 a_4 A^4)\cos(2\omega t)$ contains the even order nonlinear products. Thus, these two nonlinear terms could be used to identify the nonlinear parameters a_i. The detailed identification process is as follows. Set the input of the behavioral model as the single tone signal $x(n) = A\mathrm{e}^{j(\omega+\omega_0)n}$, according to (1), the output of the nonlinear block can be expressed as

$$s(n) = \sum_{i=1}^{N} a_i A^i \cos^i(\omega n) \tag{11}$$

By using the Fourier series expansion, the spectrum of $s(n)$ in the frequency of ω and 2ω can be expressed as Eq. (12).

$$\begin{aligned} S(\omega) &= \frac{1}{K}\sum_{n=0}^{K-1}\sum_{i=1}^{N} a_i A^i \cos^i(\omega n)\mathrm{e}^{-j\omega n} \quad \left(K = \frac{2\pi}{\omega}\right) \\ &= \sum_{i=1}^{N} a_i A^i \frac{1}{K}\sum_{n=0}^{K-1}\cos^{i+1}(\omega n) \approx \sum_{i=odd}^{N} a_i \left(\frac{A}{2}\right)^i \binom{i}{\frac{i+1}{2}} \\ S(2\omega) &= \frac{1}{K}\sum_{n=0}^{K-1}\sum_{i=1}^{N} a_i A^i \cos^i(\omega n)\mathrm{e}^{-j2\omega n} \\ &= \sum_{i=1}^{N} a_i A^i \frac{1}{K}\sum_{n=0}^{K-1}\cos^i(\omega n)\cos(2\omega n) \approx \sum_{i=even}^{N} a_i \left(\frac{A}{2}\right)^i \binom{i}{\frac{i+2}{2}} \end{aligned} \tag{12}$$

where $\binom{n}{k} = \dfrac{n!}{k!(n-k)!}$ is the binomial coefficient. Therefore, according to Eq. (6) the spectrum of the behavioral model output can be written as

$$\begin{aligned} Y_\omega(A) &= S(\omega)H(\omega) = H(\omega)\sum_{i=odd}^{N} a_i \left(\frac{A}{2}\right)^i \binom{i}{\frac{i+1}{2}} \\ Y_{2\omega}(A) &= S(2\omega)H(2\omega) = H(2\omega)\sum_{i=even}^{N} a_i \left(\frac{A}{2}\right)^i \binom{i}{\frac{i+2}{2}} \end{aligned} \tag{13}$$

where $H(\omega)$ is the frequency response function of the linear block. With the variation of input amplitude A, Equation (13) can be written in the form of matrix as

$$\mathbf{Y}_\omega = \mathbf{P}_1\boldsymbol{\alpha} \qquad \mathbf{Y}_{2\omega} = \mathbf{P}_2\boldsymbol{\beta} \tag{14}$$

in which $\boldsymbol{\alpha}$ and $\boldsymbol{\beta}$ are the vectors of odd order and even order nonlinear parameters, and $\mathbf{Y}_\omega$ and $\mathbf{Y}_{2\omega}$ are output spectrum in the frequency of ω and 2ω, respectively (assume N is odd).

$$\begin{aligned}
\mathbf{P}_1 &= H(\omega)\begin{bmatrix} \frac{A_1}{2} & \cdots & \left(\frac{A_1}{2}\right)^N \binom{N}{\frac{N+1}{2}} \\ \frac{A_2}{2} & \cdots & \left(\frac{A_2}{2}\right)^N \binom{N}{\frac{N+1}{2}} \\ \vdots & \ddots & \vdots \\ \frac{A_L}{2} & \cdots & \left(\frac{A_L}{2}\right)^N \binom{N}{\frac{N+1}{2}} \end{bmatrix}, \\
\mathbf{P}_2 &= H(2\omega)\begin{bmatrix} \left(\frac{A_1}{2}\right)^3 \binom{2}{2} & \cdots & \left(\frac{A_1}{2}\right)^{N-1} \binom{N-1}{\frac{N+1}{2}} \\ \left(\frac{A_2}{2}\right)^3 \binom{2}{2} & \cdots & \left(\frac{A_2}{2}\right)^{N-1} \binom{N-1}{\frac{N+1}{2}} \\ \vdots & \ddots & \vdots \\ \left(\frac{A_L}{2}\right)^3 \binom{2}{2} & \cdots & \left(\frac{A_L}{2}\right)^{N-1} \binom{N-1}{\frac{N+1}{2}} \end{bmatrix} \\
\boldsymbol{\alpha} &= [a_1 \quad a_2 \quad \ldots \quad a_N]^{\mathrm{T}}, \mathbf{Y}_\omega = [Y_\omega(A_1) \quad \ldots \quad Y_\omega(A_L)]^{\mathrm{T}} \\
\boldsymbol{\beta} &= [a_2 \quad a_4 \quad \ldots \quad a_{N-1}]^{\mathrm{T}}, \mathbf{Y}_{2\omega} = [Y_{2\omega}(A_1) \quad \ldots \quad Y_{2\omega}(A_L)]^{\mathrm{T}}
\end{aligned} \tag{15}$$

Therefore, the possible mean-squared-error cost function to identify the nonlinear parameters is given by

$$\hat{\boldsymbol{\alpha}} = \arg\min_{\boldsymbol{\alpha},N} \left\| \mathbf{Y}_\omega{}^{\text{measured}} - \mathbf{P}_1\boldsymbol{\alpha} \right\|^2 \qquad \hat{\boldsymbol{\beta}} = \arg\min_{\boldsymbol{\beta},N} \left\| \mathbf{Y}_{2\omega}{}^{\text{measured}} - \mathbf{P}_2\boldsymbol{\beta} \right\|^2 \tag{16}$$

where $\mathbf{Y}_\omega{}^{\text{measured}}$ and $\mathbf{Y}_{2\omega}{}^{\text{measured}}$ are the measured output spectrum, and they can be obtained in the experiment by the way of adjusting the input frequency ω to make nonlinear components in the frequencies of ω and 2ω within the output bandwidth, respectively. Thus, the nonlinear parameters vectors $\boldsymbol{\alpha}$ and $\boldsymbol{\beta}$ can be estimated by Eq. (16). In consequence, the nonlinear parameter a_i and linear parameter b_m can be well identified by the appropriate input-output data. For the nonlinear block, the accuracy of identification is much related to the optimization of Equation (16), and the model order N greatly affects computation of the optimization process. In this paper, the recursive least-squares method is used to solve these equations, and the accuracy will be validated in the experiment in next section.

4. EXPERIMENTAL VALIDATION

4.1. Test Setup

In this section, the experiment will be carried out to validate the feasibility and accuracy of the proposed behavioral model. The experiment receiver is a digital intermediate frequency receiver of Baluelec RMR200, which has a double-conversion structure of the RF front-end. The RF input range is from 20 MHz to 1.5 GHz, and IF output is 75 MHz with the bandwidth of 21.4 MHz. A test setup is constructed for the measurement as shown in Fig. 6, which includes two vector signal generators (Keysight N5166B and E8267D), an arbitrary waveform generator (RIGOL DG5351), an oscilloscope (Tektronix MSO44), a spectrum analyzer (R&S FSL18), a computer, a power combiner, and a power divider.

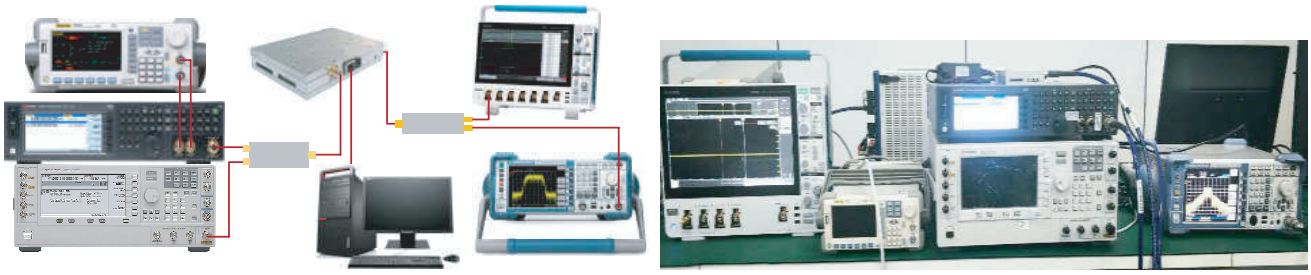

(a) (b)

Figure 6. Setup of the measurement. (a) Instruments connection diagram. (b) Picture of the experimental measurement.

In the following the procedure of parameters identification of the proposed behavioral model is summarized:

(i) Because the tuning frequency of the experimental receiver is 1000 MHz, and the IF is 75 MHz, the ω_0 in the frequency conversion block of the behavioral model can be set as 925 MHz.

(ii) For the identification of the linear parameter b_m, the sinc function is used to modulate the RF input signal to make its bandwidth cover the whole working span of the receiver. The input power is set as -50 dBm which is small enough to keep the receiver working in the linear region. Then, process the IF outputs with the spectrum analyzer (R&S FSL18) and get the output spectrum $\mathbf{Y}_\omega$. Therefore, parameter b_m can be obtained by Eqs. (7) and (8).

(iii) For the identification of nonlinear parameters a_i, the single-tone signal with sweeping power from -80 dBm to 10 dBm is used as the input. Based on the identification process in section 3.2 and $\omega_0 = 925$ MHz, set the input frequency as 1000 MHz and 960 MHz respectively to measure the IF output spectrum of 75 MHz, then the odd-order nonlinear data ${\mathbf{Y}_\omega}^{\text{measured}}$ and even-order nonlinear data ${\mathbf{Y}_{2\omega}}^{\text{measured}}$ can be obtained. According to Eq. (16), the nonlinear parameters can be estimated.

Consequently, the identification of the behavioral model of the experimental receiver front-end is implemented completely with the measurement and calculation. The process of computation and optimization is carried out in the mathematical software MATLAB, and the model parameters a_i and b_m, and the model order M and N can be determined with the measured data.

4.2. Validation

In order to evaluate the feasibility and accuracy of the proposed behavioral model, single-tone signals, multitone signals and WCDMA signals are used as the validation signals. The single-tone signal is to validate the AM-AM curve which can depict the nonlinear characteristics of receivers such as 1 dB compression point and the spurious-free dynamic range. The single-tone signals with the variation of the input power from -80 dBm to 0 dBm and the fixed frequency of 1000 MHz are generated by the signal generators (Keysight N5166B) to stimulate the experiment receiver, and then the IF output powers of 75 MHz are measured and recorded by the spectrum analyzer. Also, the same single-tone signals are used as the inputs of the behavioral model (with the order $N = 7$) to calculate the IF output. The AM/AM curves of the experiment measurement and behavioral model simulation are depicted in Fig. 7, respectively. The comparison between curves of behavioral model and the measured indicates that simulation results of the behavioral model are highly consistent with that of the measured ones, and the error is less than 0.3 dB as shown in Fig. 7.

As the analysis in Section 3, the behavioral model accuracy is very dependent on the model order N. Generally, the higher order of the model makes the greater accuracy of the nonlinear prediction, but also requires more calculation amount, and the accuracy will no longer be improved when the order exceeds a certain level. In this paper, the effect of the order N on the behavioral model accuracy is

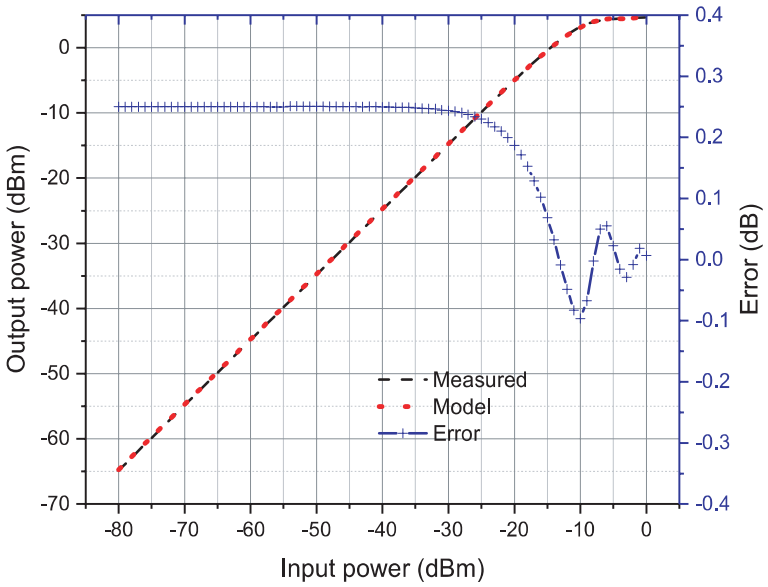

Figure 7. AM/AM curves of the measured and the behavioral model.

discussed as follows. The normalized mean square error (NMSE) is used to denote the behavior model accuracy, and it can be expressed as Equation (17).

$$\mathrm{NMSE} = 10\log_{10}\left(\frac{\sum_{i=1}^{N}|y_i-\hat{y}_i|^2}{\sum_{i=1}^{N}|y_i|^2}\right) \tag{17}$$

The NMSE of the behavioral model with the change of the model order N is shown in Fig. 8. Obviously, the NMSE falls sharply with the increase of the order and reaches a small value about -45 dB at the order of 7. When the order N is above 7, the NMSE has a small rise and then tends to

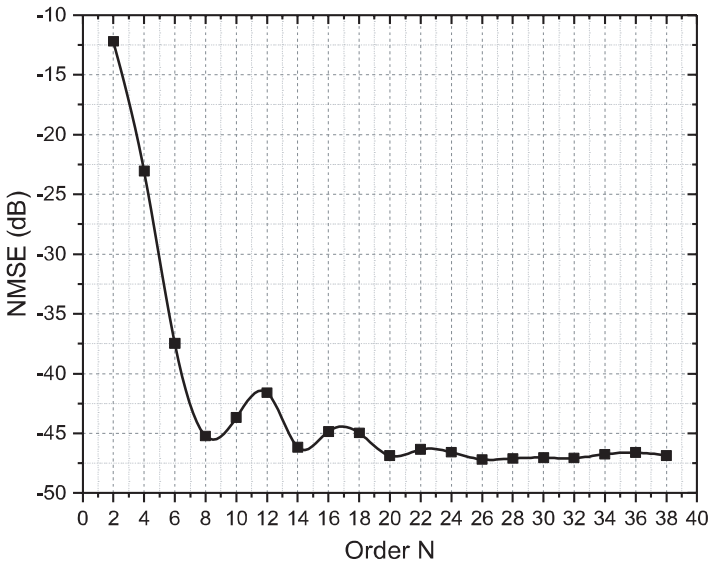

Figure 8. NMSE of the behavioral model with the order N.

be steady at −46 dB approximately. Therefore, the behavioral model has a great accuracy under the validation of single-tone signals.

The multitone signal is used to simulate the actual input with interference signals, which could give rise to the nonlinear effects such as the intermodulation and cross-modulation, and lead to signal distortion and spurious responses. To evaluate the prediction accuracy of the behavioral model on these nonlinear effects of the receiver front-end, the 10-tones signal with the range from 995 MHz to 1004 MHz and the interval of 1 MHz is generated as the input in the experiment. To produce the nonlinear effects of the receiver front-end, the input power is set as −10 dBm. The output waveforms in time domain of the measured and behavior model are shown in Fig. 9(a). We observe that the output waveforms of the behavioral model nearly overlap that of the measured one. Furthermore, to reveal the discrepancy between the waveforms clearly, the error curves are also calculated and depicted. Obviously, both error curves fluctuate within a small range. Also, the spectrum of the output is analyzed, as shown in Fig. 9(b), and the output spectrum contains not only IF components corresponding to the 10-tone input signal, but also plenty of the intermodulation products within the IF passband. The spectrum of behavioral model has slight error with that of the measured one.

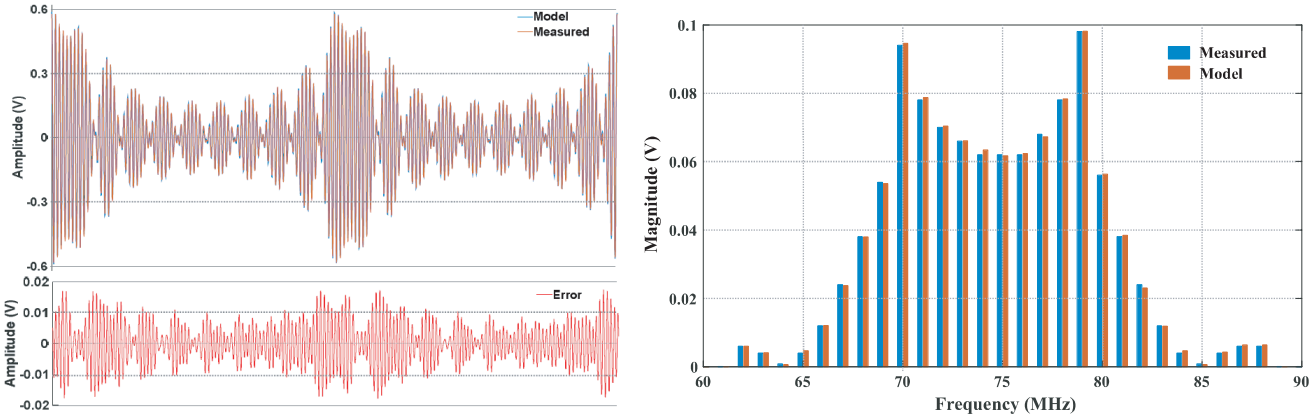

(a) (b)

Figure 9. IF output waveform and spectrum for the input of 10-tone signal with interval of 1 MHz.

With the excitation of wideband modulation signals, the memory effect of the receiver front-end is considerable, and it affects the nonlinear effects greatly. Thus, the most common wideband signal, WCDMA signal, is used to evaluate the prediction accuracy on the nonlinearities with memory effects of the proposed behavioral model. In the experiment, the standard 3GPP-FDD WCDMA signal, with the bandwidth of 5 MHz and the carrier frequency of 1000 MHz, is generated as the input, and the power spectrum density (PSD) of the IF output is measured by the spectrum analyzer. In Fig. 10, the PSD curves are depicted with the input powers of −10 dBm and −30 dBm. It is observed that the behavioral model simulation results are in good accordance with the measured data.

With the increase of the input power, due to the nonlinear effects of the receiver front-end, the adjacent channel interference becomes more and more obvious. As shown in Fig. 10, three channels, the main channel, lower adjacent channel, and upper adjacent channel, are zoned separately, and the bandwidth of each channel is set as 3.84 MHz. In order to quantitatively analyze the prediction accuracy, the main channel power and adjacent channel power are calculated respectively, as illustrated in Table 1. The error of each channel power between the measurement and model simulation is less than 0.5 dB. The comparison with the measured data shows that the channel power can be well predicted by the behavioral model.

With the validation of WCDMA signals, the comparison between the dynamic AM/AM characterizations of the behavioral model and the experimental measurement is given, as shown in Fig. 11. The dynamic AM/AM characterizations are no longer smooth curves, and these kinds of deviation reveal the time-dependent relations of the output to the input, which stands for the memory

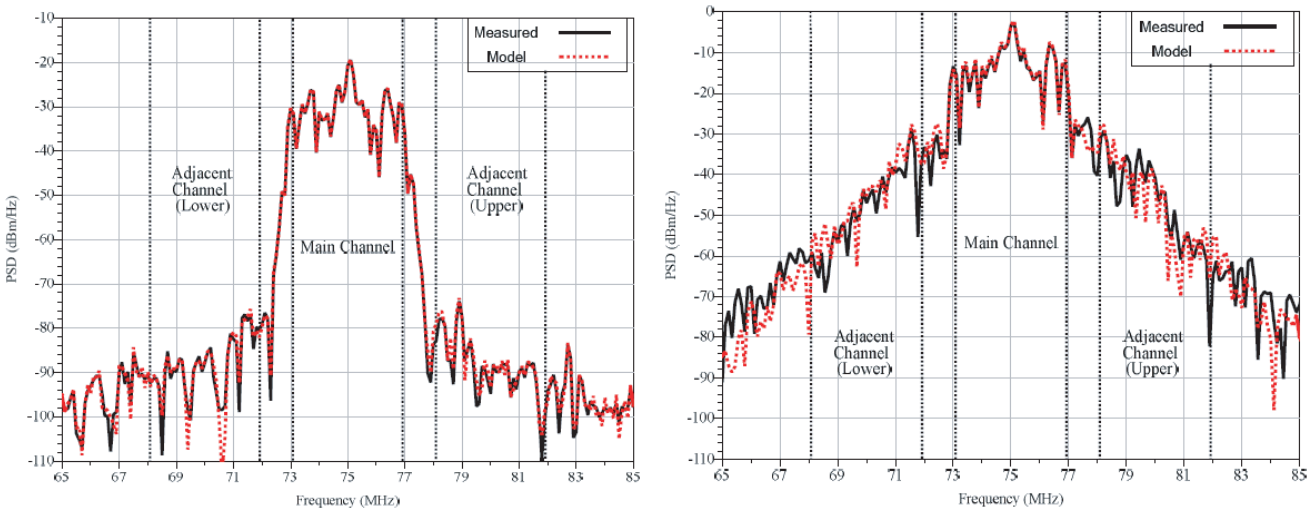

Figure 10. PSD of IF outputs with the input of WCDMA signals. (a) −30 dBm. (b) −10 dBm.

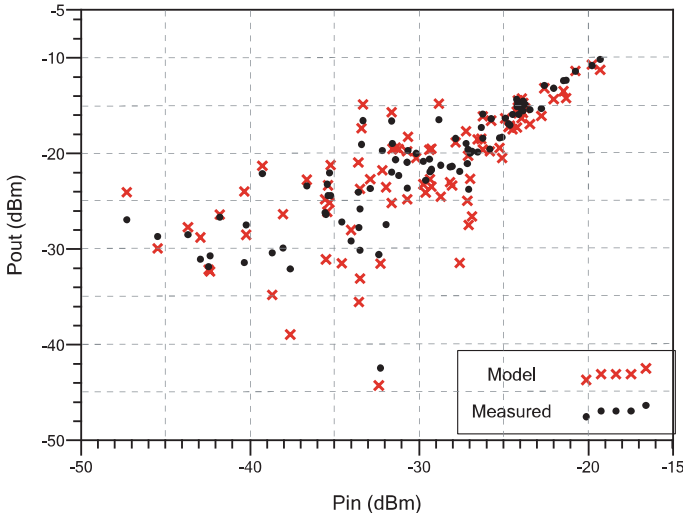

Figure 11. Dynamic AM/AM characteristic curves with the input of WCDMA signals.

Table 1. The channel powers of IF outputs.

Input Power (dBm)		Main Channel (dBm)	Adjacent Channel (dBm)	
			Lower	Upper
−30	Meas.	−12.08	−68.17	−67.96
	Model	−11.97	−68.35	−67.01
−10	Meas.	4.77	−23.23	−22.67
	Model	5.37	−21.67	−20.68

effects. The outputs corresponding to the inputs with the same amplitude will vary at different instantaneous. The relative variation range of the small signals is larger than that of the large signal, and the variation becomes smaller and smaller with the signal becoming larger. It is suggested that, for

the with nonconstant envelope signals (WCDMA signals) applied to the receiver front-end, the output of the small signal will be strongly affected by the nearby previous large signals because of the memory effects. As shown in Fig. 11, the behavioral model can well represent this kind of memory effects.

5. CONCLUSION

In this paper, a behavioral model is proposed to predict the nonlinear effects of the receiver front-end, which is significant for the EMC analysis of receivers. Since the receiver front-end is a complex nonlinear system that contains various nonlinear devices, its construction and nonlinear effects are studied comprehensively in the first place. With the analysis of the nonlinear characteristic of receiver front-end, a behavioral model with a block-oriented structure is constituted by three blocks, the frequency conversion block, memoryless nonlinear block, and memory linear block, which are used to represent the frequency conversion function, nonlinear effects, and memory effects, respectively. According to the nonlinear characteristic of receiver front-end, the identification procedures of the linear parameters and nonlinear parameters are proposed, respectively. To evaluate the feasibility and accuracy of the proposed behavioral model, a receiver of Baluelec RMR200 and the test setup are prepared for the experiment. The single-tone signals, 10-tone signals, and WCDMA signals are used as the validation signals. Under the excitation of single-tone signals, the AM/AM curves of the receiver front-end are analyzed. The error between the measurement and model simulation is small, which is much related to the model order of the behavioral model. Also, the behavioral model can accurately predict the intermodulation products of the receiver front-end with the excitation of 10-tone signals. Moreover, with the validation of WCDMA signals, the PSD distribution and dynamic AM/AM characterization of the measured and behavioral model are analyzed, and the results show that the behavioral model can well represent the nonlinearities and memory effects caused by the wideband nonconstant envelope input signals. Consequently, the behavioral model has a good accuracy of the prediction on the nonlinear effects of the receiver front-end.

REFERENCES

1. Ku, H. and J. S. Kenney, "Behavioral modeling of RF power amplifiers considering IMD and spectral regrowth asymmetries," *IEEE MTT-S International Microwave Symposium Digest*, Vol. 2, 799–802, Philadelphia, PA, USA, 2003.
2. Vuolevi, J., T. Rahkonen, and J. Manninen, "Measurement technique for characterizing memory effects in RF power amplifiers," *RAWCON 2000, 2000 IEEE Radio and Wireless Conference (Cat. No. 00EX404)*, 195–198, Denver, CO, USA, 2000.
3. Dooley, J., B. O'Brien, K. Finnerty, and R. Farrell, "Estimation of sparse memory taps for RF power amplifier behavioral models," *IEEE Microwave and Wireless Components Letters*, Vol. 25, No. 1, 64–66, Jan. 2015.
4. Carvalho, N. B., J. C. Pedro, W. Jang, and B. S. Michael, "Nonlinear simulation of mixers for assessing system-level performance," *International Journal of RF and Microwave Computer-Aided Engineering*, Vol. 15, No. 4, 350–361, Jul. 2005.
5. Mordachev, V. and E. Sinkevich, "Spurious and intermodulation response analysis of passive double-balanced mixers using the double-frequency scanning technique," *2013 International Symposium on Electromagnetic Compatibility*, 737–742, 2013.
6. Peng, S., P. J. McCleer, and G. I. Haddad, "Nonlinear models for the intermodulation analysis of FET mixers," *IEEE Transactions on Microwave Theory and Techniques*, Vol. 43, No. 5, 1037–1045, May 1995.
7. Wood, J., D. E. Root, and N. B. Tufillaro, "A behavioral modeling approach to nonlinear model-order reduction for RF/microwave ICs and systems," *IEEE Transactions on Microwave Theory and Techniques*, Vol. 52, No. 9, 2274–2284, Sep. 2004.
8. Pedro, J. C. and S. A. Maas, "A comparative overview of microwave and wireless power-amplifier behavioral modeling approaches," *IEEE Transactions on Microwave Theory and Techniques*, Vol. 53, No. 4, 1150–1163, Apr. 2005.

9. Zhu, A., M. Wren, and T. J. Brazil, "An efficient Volterra-based behavioral model for wideband RF power amplifiers," *IEEE MTT-S International Microwave Symposium Digest*, Vol. 2, 787–790, Philadelphia, PA, USA, 2003.
10. Liu, Y., J. Zhou, W. Chen, and B. Zhou, "A robust augmented complexity-reduced generalized memory polynomial for wideband RF power amplifiers," *IEEE Transactions on Industrial Electronics*, Vol. 61, No. 5, 2389–2401, May 2014.
11. Pedross-Engel, A., H. Schumacher, and K. Witrisal, "Modeling and identification of ultra-wideband analog multipliers," *IEEE Transactions on Circuits and Systems I: Regular Papers*, Vol. 65, No. 1, 283–292, Jan. 2018.
12. Root, D. E., J. Wood, N. Tufillaro, D. Schreurs, and A. Pekker, "Systematic behavioral modeling of nonlinear microwave/RF circuits in the time domain using techniques from nonlinear dynamical systems," *Proceedings of the 2002 IEEE International Workshop on Behavioral Modeling and Simulation, 2002, BMAS 2002*, 71–74, 2002.
13. Mirri, D., G. Luculano, F. Filicori, G. Pasini, G. Vannini, and G. P. Gabriella, "A modified Volterra series approach for nonlinear dynamic systems modeling," *IEEE Transactions on Circuits and Systems I: Fundamental Theory and Applications*, Vol. 49, No. 8, 1118–1128, Aug. 2002.
14. Traverso, P. A., D. Mirri, G. Pasini, and F. Filicori, "A nonlinear dynamic S/H-ADC device model based on a modified Volterra series: Identification procedure and commercial CAD tool implementation," *IEEE Transactions on Instrumentation and Measurement*, Vol. 52, No. 4, 1129–1135, Aug. 2003.
15. Wood, J. and D. E. Root, "The behavioral modeling of microwave/RF ICs using non-linear time series analysis," *IEEE MTT-S International Microwave Symposium Digest*, Vol. 2, 791–794, Philadelphia, PA, USA, 2003.
16. Grimm, M., M. Allén, J. Marttila, M. Valkama, and R. Thomä, "Joint mitigation of nonlinear RF and baseband distortions in wideband direct-conversion receivers," *IEEE Transactions on Microwave Theory and Techniques*, Vol. 62, No. 1, 166–182, Jan. 2014.